Aerosol ionic components at Mt. Heng in central southern China: Abundances, size distribution, and impacts of long-range transport

Xiaomei Gao [a], Likun Xue [b], Xinfeng Wang [a], Tao Wang [a,b,c,*], Chao Yuan [a,b], Rui Gao [a], Yang Zhou [a], Wei Nie [a], Qingzhu Zhang [a], Wenxing Wang [a,c]

[a] Environment Research Institute, Shandong University, Jinan 250100, China
[b] Department of Civil and Structural Engineering, The Hong Kong Polytechnic University, Hong Kong, China
[c] Chinese Research Academy of Environmental Sciences, Beijing 100012, China

HIGHLIGHTS

► Water-soluble ions in $PM_{2.5}$ were first investigated at Mt. Heng in southern China.
► The major factors affecting the variations of fine aerosol were identified.
► SO_4^{2-} and NH_4^+ peaked mainly in the size-bin of 0.56–1 μm, while NO_3^- in 3.2–5.6 μm.
► Aerosol at Mt. Heng showed different characteristics from those in northern China.
► Long-range transport from coastal regions dominated $PM_{2.5}$ levels in southern China.

ABSTRACT

Water-soluble ions in $PM_{2.5}$ were continuously measured, along with the measurements of many other species and collection of size-resolved aerosol samples, at the summit of Mt. Heng in the spring of 2009, to understand the sources of aerosols in rural central southern China. The mean concentrations of SO_4^{2-}, NH_4^+ and NO_3^- in $PM_{2.5}$ were 8.02, 2.94 and 1.47 μg/m^3, indicating a moderate aerosol pollution level at Mt. Heng. Water-soluble ions composed approximately 40% of the $PM_{2.5}$ mass on average. $PM_{2.5}$ was weakly acidic with about 66% of the samples being acidic. SO_4^{2-}, NO_3^- and NH_4^+ exhibited similar diurnal patterns with a broad afternoon maximum. SO_4^{2-} and NH_4^+ were mainly present in the fine aerosols with a peak in the droplet mode of 0.56–1 μm, suggesting the important role of cloud processing in the formation of aerosol sulfate. NO_3^- was largely distributed in the coarse particles with a predominant peak in the size-bin of 3.2–5.6 μm. Long-distance transport of processed air masses, dust aerosols, and cloud/fog processes were the major factors determining the variations of fine aerosol at Mt. Heng. The results at Mt. Heng were compared with those obtained from our previous study at Mt. Tai in north China. The comparison revealed large differences in the aerosol characteristics and processes between southern and northern China. Backward trajectories indicated extensive transport of anthropogenic pollution from the coastal regions of eastern/northern China and the Pearl River Delta (PRD) to Mt. Heng in spring, highlighting the need for regionally coordinated control measures for the secondary pollutants.

© 2012 Elsevier B.V. All rights reserved.

1. Introduction

Atmospheric fine particles are of major environmental concern because they adversely affect human health (Watson, 2002; Davidson et al., 2005), reduce visibility, and alter climate (Anderson et al., 2002). Fine particles are a complex mixture of various chemical constituents that can dynamically vary with time and place. Water-soluble ions generally contribute to a large portion of aerosols and determine the chemical and optical properties of aerosols by affecting their hygroscopic and

acidic natures (Ocskay et al., 2006). Thus extensive efforts have been made by scientific community to understand the temporal/spatial distributions and chemical/dynamic processes of the ionic species. In China, a number of field studies have been carried out to characterize water-soluble ions in fine aerosols (i.e., $PM_{2.5}$) in the past decade (e.g., He et al., 2001; Yao et al., 2002; Zhang et al., 2004; Wang et al., 2005; Chan and Yao, 2008; Hu et al., 2008; Yang et al., 2011). These studies have indicated a distinct spatial distribution of $PM_{2.5}$ pollution in China with high levels usually observed in the cities of the northern and western regions. Secondary water-soluble ions (i.e., SO_4^{2-}, NO_3^- and NH_4^+) typically composed a major fraction of $PM_{2.5}$ (i.e., 40%–57%) in eastern China. The previous studies were

mainly conducted in several fast developed and highly polluted regions, namely North China Plain (NCP), Yangtze River Delta (YRD) and Pearl River Delta (PRD); in comparison, little is known about the chemical characteristics and processes of aerosols in other regions, such as central southern China.

To gain understanding of aerosol pollution in central southern China, highly time-resolved and size-resolved measurements of water-soluble ions were made at Mt. Heng in the spring of 2009. This was part of the efforts of China's National Basic Research Program (the 973 Program) on acid rain pollution and control. Mt. Heng stands in the heart of China's acid rain-impacted zone that suffered from the most acidic precipitation but with less anthropogenic emissions (Xu et al., 2009). Therefore, it is of particular interest to learn about the transport of acidic substances and other pollutants including aerosols to this region from the source areas with most emissions. The geographical location of Mt. Heng makes it an ideal site to characterize the long-range transport of air pollution from both the eastern/northern China and the PRD to central southern China in spring, a transition period with northerly and southerly winds predominating in turn (see Fig. 1). In this manuscript, the measurement results of water-soluble ionic components are presented, including the acidic characteristics, diurnal patterns and size distributions. Major factors affecting the aerosol pollution at Mt. Heng and the contributions from long-range transport were also quantified. The results of this study are compared with those obtained from Mt. Tai in north China to reveal the differences in the aerosol characteristics and processes between southern and northern China.

2. Methodologies

2.1. Experimental

The measurement campaign was carried out in a meteorological station at the summit of Mt. Heng (112°42′ E, 27°18′ N, 1269 m a.s.l.) from 15 March to 31 May 2009. Mt. Heng is located in Hunan province, overlooking the PRD ~400 km to the south and the YRD ~900 km to the northeast, which are two well-known highly industrialized regions of China (see Fig. 1). The industrial zone of Hunan

province (i.e., the "Changsha–Zhuzhou–Xiangtan" city cluster) is situated about 70 km to the north. Mt. Heng is a famous tourist site that receives a lot of visitors every day. However, our measurement site is situated in the infrequently visited eastern part of the summit, and there are no large emission sources within a 50-km radius. Sun et al. (2010) have provided a detailed description of the meteorological conditions during this field campaign. In brief, spring is a transition period between the winter and summer Asian monsoons which generally control the climate of southern China. The monthly mean temperatures increased from 9.8 °C in March to 16.3 °C in May, and the southwesterly and northerly winds predominated throughout the study period.

The measurement instruments were placed in a laboratory on the second floor of the station. The sample inlets were installed at ~1.5 m above the rooftop of the station (approximately 6 m above the ground). An ambient ion monitor (AIM; Model URG-9000B, URG Co.) was deployed to measure the hourly concentrations of water-soluble inorganic ions in $PM_{2.5}$, including F^-, Cl^-, NO_2^-, NO_3^-, SO_4^{2-}, Na^+, NH_4^+, K^+, Mg^{2+} and Ca^{2+}. This analyzer has been used in our previous field studies, and the detailed descriptions have been given elsewhere (e.g., Zhou et al., 2010; Gao et al., 2011). During the entire mission, the AIM measurements started from 21 March and ended on 31 May. Multi-point calibrations were performed every four days after changing the eluent solutions. The estimated detection limits ranged from 0.010 to 0.084 μg/m^3 for all the ions, and the measurement uncertainties were approximately 10%. The positive interference for SO_4^{2-} was also found at Mt. Heng when the SO_2 concentrations were >5 ppbv for several consecutive hours, and these data were corrected based on the concurrent filter-based measurements, similar to our previous study at Mt. Tai (Zhou et al., 2010).

Size-resolved aerosol samples were collected on cloud-free days with the Micro-Orifice Uniform Deposit Impactor (MOUDI). A total of 28 sets of samples were collected during the campaign with each set comprising of nine samples in the size ranges of ≥18, 10–18, 5.6–10, 3.2–5.6, 1.8–3.2, 1.0–1.8, 0.56–1.0, 0.32–0.56 and 0.18–0.32 μm (Gao et al., 2010). These samples were then analyzed for the water-soluble ions. Mass concentrations of $PM_{2.5}$ were continuously measured by a TEOM 8500 ambient particulate monitor (Rupprecht & Patashnick Co.). O_3 was measured by a UV photometric analyzer (TEI Model 49i).
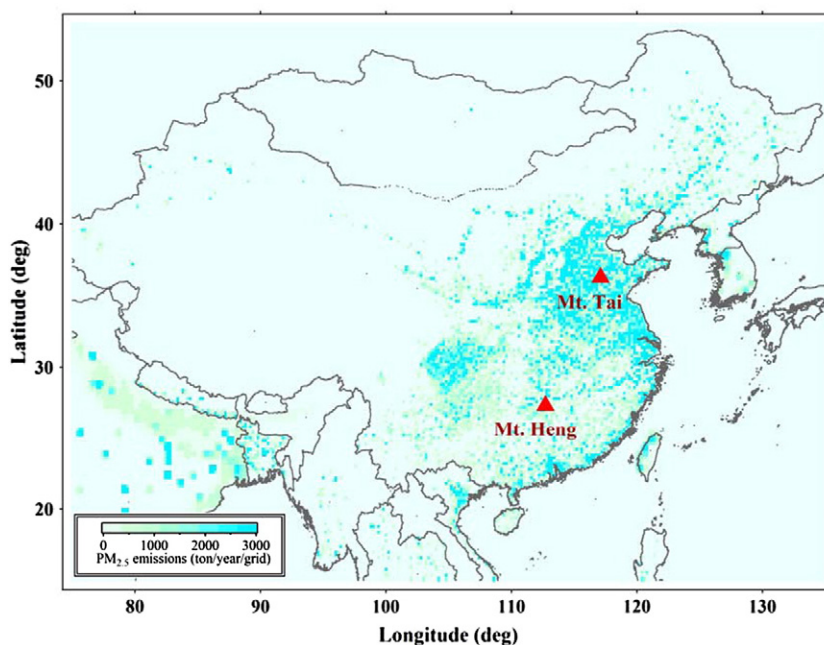

Fig. 1. Map showing the geographical location of Mt. Heng and the Asian emission inventory of PM$_{2.5}$ in 2006 (Zhang et al., 2009). The location of Mt. Tai whose data are compared against in the present study is also shown.

SO_2 was measured by a pulsed UV fluorescence analyzer (TEI, Model 43C trace level). NO and NO_2 were analyzed with a chemiluminescence instrument (TEI Model 42i) equipped with a photolytic NO_2-converter (Meteorologie consult gmbh). Black carbon (BC) was measured with a commercial Aethalometer (Magee Scientific, Model AE-21). These instruments have been widely utilized and described in our previous studies (e.g., Xue et al., 2011). The meteorological data were provided by the Mt. Heng Meteorological Station.

2.2. Backward trajectory calculation and cluster analysis

To learn about the origins and transport histories of air masses sampled at Mt. Heng, we computed the three-dimensional five-day backward trajectories terminating at the height of 1300 m a.s.l. every hour for the study period. The Hybrid Single-Particle Lagrangian Integrated Trajectory model (HYSPLIT; version 4.9) was used for the calculation with the Global Data Assimilation system (GDAS) data as meteorological inputs (Draxler and Rolph, 2003). A total of 1872 trajectories were obtained. A hierarchical cluster approach was then utilized to classify these trajectories into several different groups based on the Ward's cluster method with a squared Euclidean measure. The positions (i.e., longitude, latitude and pressure) of the 120 hourly endpoints along each trajectory were selected as the clustering variables. The computation was performed on a computer using the statistical software SPSS. This approach has been employed in our previous studies at other mountainous sites (Wang et al., 2006; Xue et al., 2011).
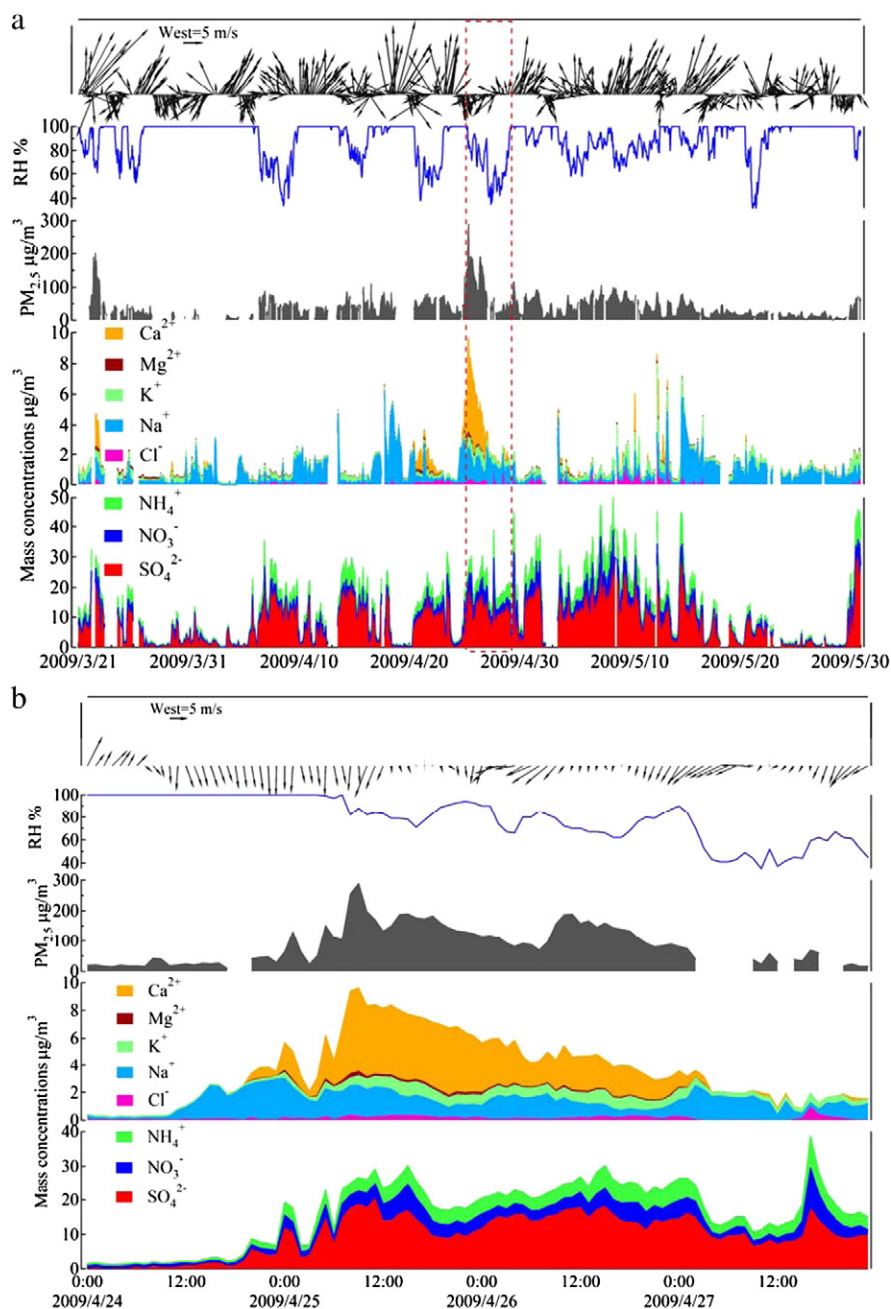

Fig. 2. Time series of $PM_{2.5}$, major water-soluble ions, and meteorological parameters at Mt. Heng during (a) the whole study period and (b) the dust event on 25–26 April, 2009.

3. Results and discussion

3.1. Overview of measurement data

3.1.1. Water-soluble ions in $PM_{2.5}$

Fig. 2a depicts the time series of $PM_{2.5}$, its water-soluble ions, and meteorological parameters measured at Mt. Heng from 21 March to 31 May 2009. From this figure, it can be clearly seen that both multi-day clean periods and moderate pollution events appeared in turn during the study period, with the pollutant concentrations varying in a wide range. The clean periods generally started with the onset of clouds/fogs or rainfalls which rapidly scavenged most pollutants and usually lasted for several days, and remained till the rainfalls and clouds/fogs stopped. After that, the pollutant concentrations began increasing gradually to reach moderate to high pollution levels. In particular, secondary water-soluble ions (i.e., SO_4^{2-}, NO_3^- and NH_4^+) were evidently formed and accumulated during these pollution events.

Table 1 summarizes the statistics of $PM_{2.5}$, major water-soluble ions, and related trace gasses for the whole dataset and for subsets of measurements on the cloudy and cloud-free period. Overall, moderate aerosol pollution was illustrated especially during the non-cloudy measurements. During the campaign, the average concentration ($\pm$ standard deviation) of $PM_{2.5}$ was 38.4 ($\pm$ 32.1) μg/m^3, which is more than twice the annual US National Ambient Air Quality Standard of $PM_{2.5}$ (15 μg/m^3). Water-soluble ions contributed to approximately 40% of the measured $PM_{2.5}$ mass. Among them, SO_4^{2-} was the most abundant composition with a mean value of 8.02 ($\pm$ 6.84) μg/m^3, followed by NH_4^+ and NO_3^- with average concentrations of 2.94 ($\pm$ 2.47) and 1.47 ($\pm$ 1.60) μg/m^3. These three species together composed about 82% of the total measured water-soluble ions. In comparison, other ions normally presented very low concentrations accounting for a minor fraction of $PM_{2.5}$ water-soluble compositions.

Table 2 compares the levels of SO_4^{2-}, NO_3^- and NO_3^-/SO_4^{2-} mass ratio at Mt. Heng with those obtained from other high-elevation sites in the world. The SO_4^{2-} and NO_3^- levels in $PM_{2.5}$ at Mt. Heng were substantially higher than those measured at mountainous locations in the US, Europe and Japan, and comparable to those observed at Mt. Hua in central China. They were also higher than the concentrations detected in the coarser particles (e.g., PM_{10} or TSP) at some remote areas of China such as Zhuzhang, Akdala and Waliguan. However, they were significantly lower compared to the levels observed at Mt. Tai in north China. During our study at Mt. Tai in the spring of 2007, very high concentrations were also observed for most other pollutants (Zhou et al., 2010; Wang et al., 2011b). For instance, the mean mixing ratios of SO$_2$ and NO$_x$ (major precursors of SO_4^{2-} and NO_3^-) were 15.4 and 4.9 ppbv respectively at Mt. Tai, compared to those of 2.0 and 1.0 ppbv at Mt. Heng in this study. This indicated that the air pollution in north China plain was much more serious than central southern China. An interesting phenomenon was that the NO_3^-/SO_4^{2-} ratio at Mt. Heng (~0.18) was also much smaller than that of Mt. Tai (~0.46), implying the atmospheric conditions of Mt. Heng may be unfavorable to the formation of fine nitrate. We will discuss the formation pathways of nitrate aerosols in Section 3.3.

3.1.2. Aerosol acidity

Aerosol acidity is an important property of particles, determining their capacity of facilitating the heterogeneous reactions on the aerosol surfaces (Underwood et al., 2001; Jang et al., 2002). In the present study, we adopted the approach of Zhou et al. (2012) to evaluate the acidic characteristics of $PM_{2.5}$ based on the hourly concentrations of SO_4^{2-}, NO_3^- and NH_4^+. These three species were selected because they normally contributed to the majority of water-soluble ions in $PM_{2.5}$ (e.g., >90%) and thus dominated its acidity. However, this method was not valid under some conditions, including several dust cases when mineral ions (e.g., Ca^{2+}, Mg^{2+}, Na^+, etc.) contributed to a large fraction of $PM_{2.5}$ and cloud/fog events when all the ions presented very low concentrations. These data were excluded from this analysis. On this basis, a total of 783 hourly data were subject to the aerosol acidity estimation, accounting for ~50% of the total valid measurements.

Fig. 3 shows the neutralization extent of SO_4^{2-} and NO_3^- by NH_4^+ ($F = NH_4^+ / (2SO_4^{2-} + NO_3^-)$). Table 3 gives the statistics of the strong acidity (H^+_{strong}), in-situ acidity (H^+_{air}) and pH of $PM_{2.5}$ at Mt. Heng. The majority of $PM_{2.5}$ samples (~66%) at Mt. Heng showed an acidic nature ($F < 0.90$), with about 44% and 22% being weakly ($F = 0.75–0.90$) and more acidic ($F < 0.75$). The average concentrations of H^+_{strong} and H^+_{air} (computed by the thermodynamic Aerosol Inorganic Model II (AIM-II)) (Clegg et al., 1998; Zhou et al., 2012) were 53.4 and 13.3 nmol/m^3 respectively, which were much lower than those of Mt. Tai (i.e., 111.5 and 25.3 nmol/m^3 in spring and 180.0 and 35.3 nmol/m^3 in summer). Examination of the chemical compositions in the $PM_{2.5}$ droplets (from the outputs of the AIM-II model) revealed that much higher concentrations of HSO_4^- and NO_3^- at Mt. Tai freed more H^+ in the liquid phase of aerosols, making $PM_{2.5}$ more acidic. An interesting finding was that fine aerosols at Mt. Heng were less acidic than that of Mt. Tai but the clouds and precipitations presented an opposite trend (Sun et al., 2010). This implied that the in-cloud and/or below-cloud scavenge processing of coarse particles and gasses may be responsible for the more acidic depositions at Mt. Heng.

Table 1
Statistics of major water-soluble ions in $PM_{2.5}$ and related parameters measured at Mt. Heng from 21 March to 31 May in 2009.

Species	All data				Non-cloudy period[a]				Cloudy period[a]			
	Mean ($\pm$SD)	Min	Max	n	Mean ($\pm$SD)	Min	Max	n	Mean ($\pm$SD)	Min	Max	n
$PM_{2.5}$ (μg/m^3)	38.4 ± 32.1	0.68	289.2	1350	50.5 ± 33.4	4.9	289.2	844	18.2 ± 15.6	0.68	116.35	506
SO_4^{2-} (μg/m^3)	8.02 ± 6.84	–	31.68	1556	12.40 ± 5.49	0.42	31.68	898	2.04 ± 2.75	–	21.64	658
NO_3^- (μg/m^3)	1.47 ± 1.60	–	12.07	1556	2.18 ± 1.62	–	12.07	898	0.50 ± 0.93	–	9.78	658
Cl^- (μg/m^3)	0.10 ± 0.18	–	2.65	1556	0.14 ± 0.20	–	2.65	898	0.03 ± 0.11	–	1.82	658
NH_4^+ (μg/m^3)	2.94 ± 2.47	0.1	13.62	1556	4.37 ± 2.14	0.31	11.57	898	0.99 ± 1.27	0.1	13.62	658
Na^+ (μg/m^3)	0.69 ± 0.82	–	6.21	1553	0.67 ± 0.81	0.04	5.34	895	0.72 ± 0.85	–	6.21	658
K^+ (μg/m^3)	0.33 ± 0.29	–	4.61	1556	0.43 ± 0.32	0.07	4.61	898	0.19 ± 0.14	–	1.55	658
Ca^{2+} (μg/m^3)	0.16 ± 0.64	–	6.11	1556	0.27 ± 0.83	–	6.11	898	0.02 ± 0.12	–	1.95	658
Mg^{2+} (μg/m^3)	0.05 ± 0.05	–	0.32	1556	0.06 ± 0.05	–	0.32	898	0.03 ± 0.03	–	0.14	658
SO_2 (ppbv)	2.02 ± 2.42	–	21.99	1664	2.83 ± 2.54	–	20.88	942	0.96 ± 1.77	–	21.99	722
NO_2 (ppbv)	1.01 ± 0.80	0.17	9.11	791	0.96 ± 0.81	0.22	9.11	551	1.12 ± 0.75	0.17	3.95	240
O_3 (ppbv)	58.8 ± 16.1	15.6	114.6	1575	67.1 ± 14.1	27.8	114.6	869	48.5 ± 12.2	15.6	97.1	706
Temp (°C)	13.3 ± 4.8	0.9	24.4	1704	15.2 ± 3.9	3.4	24.4	949	11.1 ± 5.0	0.9	18.6	755
RH (%)	88.7 ± 15.7	32	100	1704	79.7 ± 16.1	32	100	949	99.9 ± 0.7	89	100	755

"SD" is the standard deviation.
"n" is the number of hourly data.
"–" means the value below the detection limit.
[a] The cloudy samples were based on the sampling periods of cloud water samples (Sun et al., 2010).

Table 2
Comparison with other mountain sites.[a]

Location	Elevation (m a.s.l.)	Sampling period	Size	SO_4^{2-}	NO_3^-	NO_3^-/SO_4^{2-}	References
Mt. Heng, China (27.3°N, 112.7°E)	1269	Mar–May, 2009	$PM_{2.5}$	8.02	1.47	0.18	This study
Mt. Tai, China (36.3°N, 117.1°E)	1534	Mar–Apr, 2007	$PM_{2.5}$	12.76	5.81	0.46	Zhou et al. (2010)
Mt. Hua, China (34.8°N, 110.1°E)	2060	Mar–Apr, 2009	$PM_{2.1}$	8.95	1.71	0.19	Wang et al. (2011a)
Mt. Tateyama, Japan (36.6°N, 137.6°E)	3015	Spring, 1996–2000	$PM_{2.1}$	2.39	0.24	0.1	Kido et al. (2001)
San Gorgonio, USA (34.1°N, 116.9°W)	1705	Apr, 2003	$PM_{2.5}$	0.61	3.19	5.23	Lee et al. (2008)
Grand Canyon N.P., USA (36.2°N, 111.9°W)	2267	May, 2003	$PM_{2.5}$	1.03	0.26	0.25	Lee et al. (2008)
Mt. Zeppelin, Finland (78.5°N, 11.5°E)	470	Apr–May, 2001	$PM_{2.5}$	1.12	0.02	0.01	Teinilä et al. (2004)
Zhuzhang, China (28.0°N, 99.7°E)	3583	Jul, 2004–Mar, 2005	PM_{10}	1.6	0.45	0.28	Qu et al. (2009)
Akdala, China (47.1°N, 88.0°E)	562	Jul, 2004–Mar, 2005	PM_{10}	3.3	0.58	0.18	Qu et al. (2009)
Mt. Shivalik, India (29.4°N, 79.5°E)	1950	2005–2008	TSP	4.41	0.63	0.14	Ram et al. (2010)
Waliguan, China (36.3°N, 100.9°E)	3816	Oct, 1994	TSP	0.22	0.24	1.09	Yang et al. (1996)

[a] All data are the mean values. The units are µg/m³ for SO_4^{2-} and NO_3^-. The NO_3^-/SO_4^{2-} denotes the mass ratio.

To investigate the possible influence of aerosol acidity on secondary organic aerosols (SOA) formation, we estimated the secondary organic carbon (SOC) contents of $PM_{2.5}$ at Mt. Heng and Mt. Tai using the widely-adopted EC-tracer method. It estimates the SOC concentrations from the relationship of OC (organic carbon) and EC (elemental carbon) assuming a fixed ratio of OC/EC for the primary sources in the study region (Strader et al., 1999). The details of this approach have been described elsewhere (Wang et al., 2012). The mean level of SOC in $PM_{2.5}$ at Mt. Heng was estimated to be 1.85 µg/m³, which only composed about 5.9% of the measured $PM_{2.5}$ mass. In comparison, the abundances of SOC at Mt. Tai were substantially higher with mean concentrations of 8.54 and 13.78 µg/m³ in spring and summer, accounting for ~13.6% and ~23.2% of the $PM_{2.5}$ mass (Wang et al., 2012). Although there are many factors influencing the abundances of SOC in $PM_{2.5}$, higher aerosol acidity was believed as an important parameter contributing to more SOA formation at Mt. Tai (Zhang et al., 2007; Zhou et al., 2012).

3.1.3. Diurnal variations

Fig. 4 shows diurnal profiles of SO_4^{2-}, NO_3^-, NH_4^+, and related trace gasses as well as meteorological parameters at Mt. Heng. All these pollutants exhibited diurnal patterns with higher concentrations during the daytime compared to lower levels at night. These distributions were similar to those observed at Mt. Tai (Zhou et al., 2010), and can
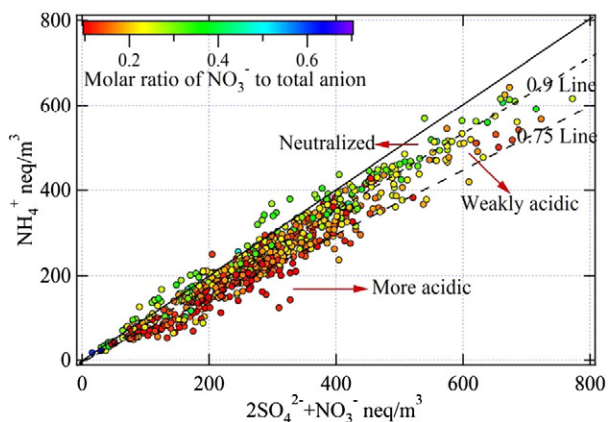
be attributed to the dynamic transport of air pollution related to mountain–valley breezes and convective mixing within the planetary boundary layer (PBL). During the daytime, the upslope winds along the mountain ridge and enhanced vertical mixing within the uplifting PBL transported the polluted air masses from the lowland areas to the summit, while the catabatic winds together with suppressed PBL could bring clean free tropospheric air to the measurement station at night. All major secondary pollutants, such as SO_4^{2-}, NO_3^- and NH_4^+, showed a broad afternoon maximum pattern. Their precursors, such as SO_2 and NO_2, also exhibited broad daytime peaks but tended to reach the maximums in the morning, a little earlier. This indicated the in-situ production of SO_4^{2-} and NO_3^- (also NH_4^+) at Mt. Heng during the daytime when the atmospheric photochemistry was active.

3.2. Processes affecting aerosol pollution at Mt. Heng

To unravel the factors/processes influencing the aerosol pollution at Mt. Heng, a principal component analysis (PCA) was applied to the measurement data collected in this study (Zhou et al., 2010). Hourly data of nss-SO_4^{2-}, NO_3^-, NH_4^+, Cl^-, Na^+, K^+, Mg^{2+}, Ca^{2+}, NO_y, SO_2, O_3 and RH were used for the PCA analysis. Five components were finally identified and could explain 81% of the total variance. The factor loadings and percentage of the variance explained by each component is shown in Table 4. The principal component 1 showed high factor loadings for NH_4^+, nss-SO_4^{2-}, NO_3^- and O_3 ($R>0.70$), and moderate loadings for SO_2, NO_y, K^+ and Cl^-. These species are either secondary pollutants or anthropogenic tracers, indicating that this component was associated with the long-range transport of

Fig. 3. Neutralization extent of SO_4^{2-} and NO_3^- by NH_4^+ in $PM_{2.5}$.

Table 3
The acidity of $PM_{2.5}$ modeled by AIM-II in $PM_{2.5}$ at Mt. Heng and Mt. Tai.

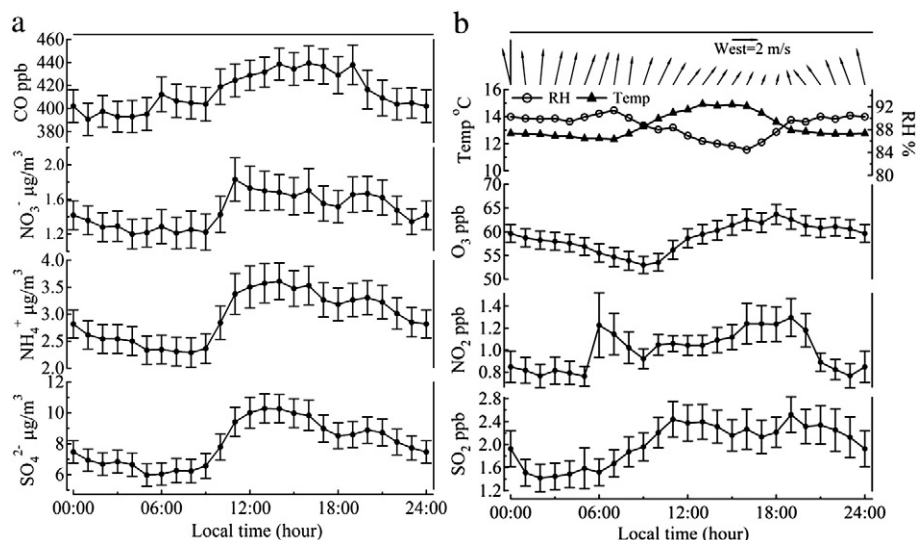|	Mt. Heng	Mt. Tai	
	Spring	Spring	Summer
Valid number	685	214	339
H^+_{air} (nmol/m³)	13.3 ± 15.4	25.3 ± 32.2	35.3 ± 30.9
H^+_{strong} (nmol/m³)	53.4 ± 38.7	111.5 ± 82.6	180.0 ± 104.4
pH	0.64 ± 0.96	−0.32 ± 1.38	−0.04 ± 1.01
HSO_4^- (nmol/m³)	35.6 ± 26.7	67.7 ± 57.7	121.3 ± 79.1
SO_4^{2-} (nmol/m³)	80.2 ± 57.8	79.8 ± 79.9	137.6 ± 121.3
NO_3^- (nmol/m³)	34.7 ± 25.7	109.1 ± 81.3	83.3 ± 60.9
Water content (µg/m³)	67.7 ± 143.3	47.9 ± 77.1	78.6 ± 137.0

Fig. 4. Average diurnal profiles of SO_4^{2-}, NO_3^-, NH_4^+, and some related parameters at Mt. Heng. The error bars indicate the standard errors of the measurement data.

chemically processed air masses influenced by anthropogenic emissions. This component showed the highest percentage with ~44% of the variance explained.

The principal component 2 was primarily comprised of Ca^{2+} and Mg^{2+} ($R > 0.80$), and thus was attributed to the crustal and soil sources. This component explained 14% of the total variance, and mainly corresponded to several cases of dust storm. A heavy dust storm attacked Mt. Heng on 25–26 April, with the observed hourly $PM_{2.5}$ and PM_{10} concentrations reaching up to 289 and 911 μg/m³ (see Fig. 2b). The concentrations of Ca^{2+}, an indicator of mineral aerosols, also increased significantly with a mean level of 3.14 μg/m³ that was much higher than those recorded on the other days (mean = ~0.03 μg/m³). Other ions such as K^+, Cl^-, SO_4^{2-}, NO_3^- and NH_4^+ also showed elevated concentrations during this dust episode, implying that the air parcels had picked up some anthropogenic pollution during transport to the measurement site.

The principal component 3 showed negative or little correlation with most species but exhibited a high positive correlation with RH ($R = 0.89$), suggesting it was related to the cloud/fog processes. This component explained ~10% of the total variance. Indeed, cloud/fog events were frequently observed during the study period (Sun et al., 2010). Consequently, cloud/fog processing was believed to play an

important role in cleaning the pollutants at Mt. Heng. On the other hand, cloud processing can also effectively transfer the acidic substances from aerosols to the clouds and/or precipitations, and thus contributes to the acid deposition in this region.

The principal component 4 grouped K^+ and Cl^- together ($R > 0.70$), which explained 8% of the total variance. K^+ is enriched in the aerosol form biomass burning (Wang et al., 2005), thus this factor was identified as biomass burning. The principal component 5 only showed a high loading for Na^+ with a variance of 5%, which may be related to sea-salt.

3.3. Size distribution and formation pathways of secondary ions

Fig. 5 shows the size profiles of SO_4^{2-}, NO_3^- and NH_4^+ measured at Mt. Heng, with measurements on the dust events excluded. SO_4^{2-} and NH_4^+ mainly existed in the fine particles with fractions of 94% and 96% being presented in $PM_{1.8}$ (note that there is no 2.5 μm cut point for MOUDI). Both species exhibited a single peak in the size-bin of 0.56– 1 μm, corresponding to the droplet mode. This was slightly different from the profiles observed at Mt. Tai in the spring of 2007 which showed the maximum in the size-range of 0.32–0.56 μm (condensation mode), but similar to those measured in summer (Gao et al., 2010). Typically, SO_4^{2-} in different sizes is formed in the atmosphere via different chemical processes. The condensation mode SO_4^{2-} is commonly formed by the heterogeneous condensation of SO_2 or H_2SO_4 on the existing particles, while SO_4^{2-} of droplet mode is usually produced by the oxidation of SO_2 in the cloud droplets (Mather et al., 2003; Roger et al., 2009; Guo et al., 2010). It appears that SO_4^{2-} was mainly formed through the gas-to-particle condensation reactions in spring at Mt. Tai, while the cloud/fog processing played a principal role at Mt. Heng. This could be ascribed to the differences in the meteorological conditions at both locations: the springtime meteorological regime at Mt. Tai was characterized by the relatively lower RH and less clouds/fogs, whereas that of Mt. Heng was featured by higher RH and frequent clouds/fogs.

At Mt. Heng, NO_3^- was largely presented in the coarse particles with about 36% and 64% being in $PM_{1.8}$ and $PM_{>1.8}$, respectively. It displayed a bimodal distribution with a predominant peak in the coarse mode of 3.2–5.6 μm and a secondary peak in the fine mode of 0.56–1 μm. This was quite different from the results obtained at Mt. Tai which showed that NO_3^- was almost equally distributed in the fine and coarse particles in both spring and summer (Gao et al., 2010). This was also in line with the result that the NO_3^-/SO_4^{2-} ratio in $PM_{2.5}$ was much lower at Mt. Heng than Mt. Tai. Generally, the

Table 4
Factor loadings from principal component analysis.

Species	Components				
	1	2	3	4	5
NH_4^+	**0.97**				
Nss-SO_4^{2-}	**0.93**				
NO_3^-	**0.89**			0.20	
O_3	**0.74**		−0.51		
NO_y	**0.55**				
SO_2	**0.47**				
Mg^{2+}		**0.88**			
Ca^{2+}		**0.85**			
RH	−0.32		**0.89**		
Cl^-	**0.51**			**0.76**	
K^+	**0.50**			**0.73**	
Na^+					**0.99**
Variance	44%	14%	10%	8%	5%

The bold and underlined values indicate loading factors discussed in this paper.
Extraction method: principal component analysis.
Rotation method: Quartimax with Kaiser Normalization. Rotation converged in 6 iterations.
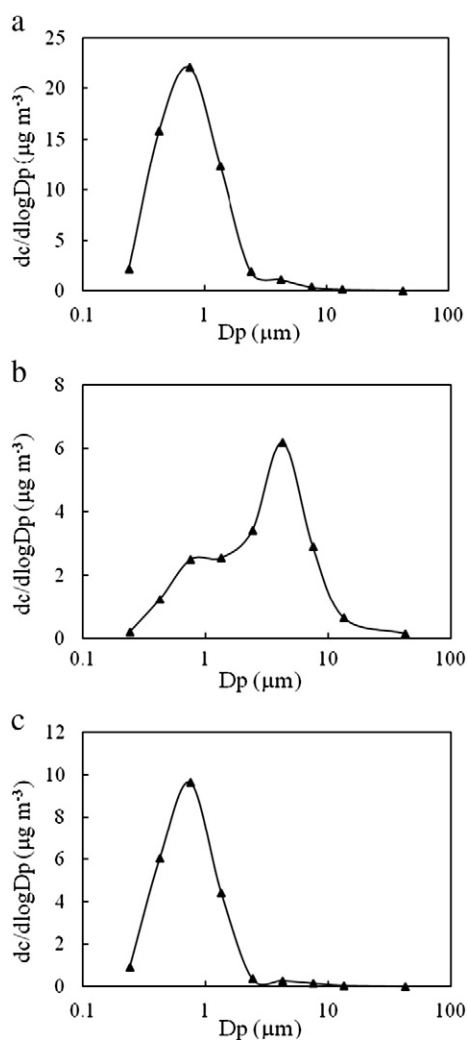
Fig. 5. Average size distributions of (a) SO_4^{2-}, (b) NO_3^- and (c) NH_4^+ at Mt. Heng on the basis of 20 sets of samples with the samples collected during the dust events being excluded.

fine NO_3^- is mainly produced through the gas phase reactions of HNO_3 with NH_3, whereas the coarse NO_3^- is generated by the condensation of HNO_3 on the surfaces of sea salt or mineral particles (Seinfeld and Pandis, 2006). Both formation pathways compete in the atmosphere with the relative availabilities of the corresponding neutralizer (i.e., NH_3 vs. coarse alkaline particles) as the major limiting factor. At Mt. Heng, NH_4^+ was not enough to neutralize the SO_4^{2-} and NO_3^- in the fine aerosols (see Fig. 3), suggesting that the shortfall of NH_3 may be the restrictive factor to the formation of fine NO_3^-.

3.4. Impacts of long-range transport

As discussed above, the long-range transport of aged air masses played a dominant role in the air pollution at Mt. Heng. To understand the transport characteristics of air masses and its impacts on the aerosol pollution, we calculated the three-dimensional five-day backward trajectories every hour for the study period and then classified them into five different groups based on the transport directions and speeds in both the horizontal and vertical scales (Xue et al., 2011). Fig. 6 shows the mean transport pathway and the percentage of each air mass category identified. The five air mass categories are: NG, continental air masses coming from the north, originated from the Gobi areas (i.e., Siberia and Mongolia) and passing over north China at higher altitudes with a high speed; NWC, another type of

continental air masses originated from the northwest China and moving slowly over central China; NEC, air masses coming from the northeast and passing in the boundary layer over the coastal regions of northern and eastern China; PRD, air masses coming from the southeast and passing over the PRD region at lower altitudes; SEA, air masses originated from southeast (SE) Asia and passing over the southwest regions of China. Note that the NEC air masses passed over the densely populated and highly industrialized NCP and YRD regions before arriving at Mt. Heng, and the PRD air masses passed over the PRD region. Therefore, these two types of air masses may be strongly influenced by anthropogenic pollution in the three regions. Among the five groups, NEC and PRD appeared the most, both of which account for 28% of the total air masses sampled. NWC also contributed considerably (24%) to the air parcels sampled in the present study with NG and SEA contributing to 15% and 5% of the total air masses, respectively. The back trajectory results indicate extensive transport of anthropogenic pollution from the northern/eastern China and the PRD regions to central southern China in the spring season.

The chemical compositions of each air mass type were examined by sorting the hourly data on major $PM_{2.5}$ water-soluble ions and related trace gasses according to the trajectory clusters. The data collected on the rainy and cloudy/foggy days were excluded here as the concentrations of most species were very low which may mask the actual pollution characteristics of the air masses. The statistical results are given in Table 5. The highest concentrations of SO_4^{2-}, NO_3^-, NH_4^+ and Cl^- were observed in the PRD category with relatively higher levels of other ions and gasses. The sum of SO_4^{2-}, NO_3^- and NH_4^+ accounted for the highest percentage in $PM_{2.5}$ (46%±12%) in this category and this category had the highest values of SOR and NOR (namely the fine sulfate and nitrate oxidation ratios, respectively). These results indicated that the air masses from PRD were significantly aged and influenced by the anthropogenic emissions. The NEC category had the secondary highest levels of pollutants with the secondary ions' percentage of 44%±13%. As these two categories accounted more than half of the total air masses, the pollution in spring at Mt. Heng was strongly affected by the transport of anthropogenic pollution from the coastal regions of eastern/northern China and the Pearl River Delta in the South.

In comparison, the continental NG and NWC air masses contained elevated concentrations of Ca^{2+}, in particular the NG that was affected by dust storms. Examination of the data revealed that the NG air masses were mainly encountered during several dust storm cases, corresponding to the fast southward export of dust plumes from the northern desert areas in spring. These air masses also showed some signatures of anthropogenic pollution with relatively high concentrations of SO_4^{2-}, NO_3^- and NH_4^+, indicating the heterogeneous reactions of acidic gasses on the mineral surfaces during transport of dust passing over high emissions regions (Heibei, Shanxi). However, the percentage of the total measured water-soluble ions in $PM_{2.5}$ was the lowest (39%±14%) (mean±standard deviation), reflecting more water insoluble species in the dust particles. The SEA air masses had the lowest concentrations of $PM_{2.5}$ and most water-soluble species but with the highest level of K^+, implying the impacts of biomass burning in SE Asia. Previous studies have shown the intensive burning of biomass in spring in SE Asia (e.g., Liu et al., 1999). It is worth noting that the frequency of this group was very low (~5%), and the air masses were mainly encountered at the beginning of the campaign (i.e., 15–21 March). The AIM measurements were commenced on 21 March, only covering the end of the plume.

4. Summary

To understand the chemical signatures and sources of aerosol pollution in central southern China, highly time- and size-resolved measurements of water-soluble ions were made at Mt. Heng in the spring
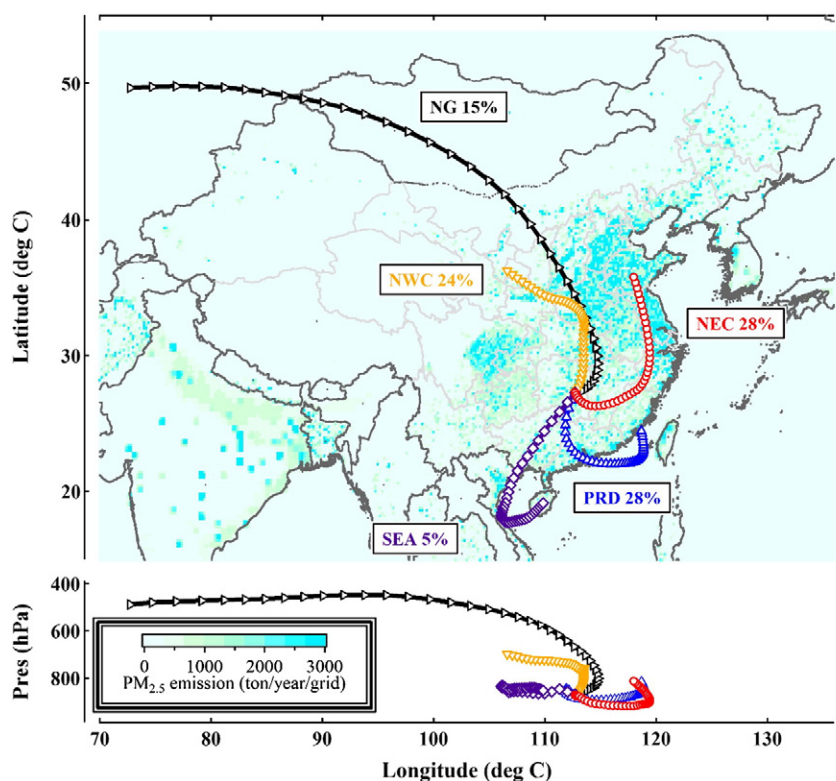
Fig. 6. Mean five-day backward trajectory clusters plotted on the Asian anthropogenic emissions of PM$_{2.5}$ in 2006 (Zhang et al., 2009). The open circles along the trajectories indicate 6-hour intervals.

of 2009. Moderate pollution levels and weakly acidic nature of PM$_{2.5}$ were indicated. Long-distance transport of aged air masses, dust/crustal sources, and cloud/fog processing were the major factors affecting the aerosol pollution. Strong transport of Asian dust storm to central southern China was observed. SO$_4^{2-}$ and NH$_4^+$ were mainly presented in the fine aerosols with a peak in the droplet mode, while NO$_3^-$ was largely existed in the coarse particles. A comparison with the results at Mt. Tai revealed large differences in the aerosol characteristics and processes between southern and northern China. In spring, back trajectory analysis revealed extensive transport of anthropogenic pollution from coastal regions of eastern China (i.e., PRD, YRD and NCP) to central southern China. The results demonstrate the importance of long-range transport in shaping secondary pollution and highlight the need for regionally coordinated control strategies in their mitigations.

Acknowledgments

Table 5
Chemical compositions (mean value ± standard deviation) of the five air mass groups at Mt. Heng.

Species	PRD	NEC	NWC	NG	SEA
PM$_{2.5}$ (μg/m³)	48.8 ± 20.7	52.5 ± 20.8	49.8 ± 43.1	52.0 ± 41.3	28.5 ± 8.6
SO$_4^{2-}$ (μg/m³)	14.26 ± 5.94	14.05 ± 5.92	11.29 ± 5.01	10.88 ± 3.77	6.53 ± 1.27
NO$_3^-$ (μg/m³)	2.69 ± 1.80	2.54 ± 1.46	1.51 ± 1.46	2.19 ± 1.51	1.65 ± 0.51
NH$_4^+$ (μg/m³)	5.33 ± 2.29	5.13 ± 2.20	3.60 ± 1.92	3.72 ± 1.45	2.93 ± 0.47
Cl$^-$ (μg/m³)	0.25 ± 0.29	0.14 ± 0.18	0.08 ± 0.11	0.13 ± 0.15	0.05 ± 0.06
K$^+$ (μg/m³)	0.51 ± 0.52	0.40 ± 0.25	0.40 ± 0.21	0.38 ± 0.19	0.52 ± 0.09
Ca^{2+} (μg/m³)	0.04 ± 0.24	0.04 ± 0.13	0.40 ± 1.09	0.63 ± 1.12	0.03 ± 0.10
Na$^+$ (μg/m³)	0.86 ± 1.11	0.43 ± 0.49	0.71 ± 0.74	0.67 ± 0.66	0.36 ± 0.32
SO$_2$ (ppbv)	2.35 ± 2.92	3.24 ± 2.66	2.58 ± 2.00	3.71 ± 2.45	1.03 ± 1.00
NO$_y$ (ppbv)	4.31 ± 2.02	4.52 ± 2.26	3.90 ± 2.15	3.95 ± 2.20	3.50 ± 0.58
SOR	0.63 ± 0.21	0.50 ± 0.17	0.50 ± 0.16	0.40 ± 0.12	0.62 ± 0.17
NOR	0.18 ± 0.08	0.17 ± 0.08	0.10 ± 0.06	0.16 ± 0.06	0.14 ± 0.04
N	244	194	286	192	33

SOR = Nss − SO$_4^{2-}$/(Nss − SO$_4^{2-}$ + SO$_2$), NOR = NO$_3^-$/NO$_y$, N is the number of trajectories for each air mass type.

References

Anderson RR, Martello DV, Rohar PC, Strazisar BR, Tamilia JP, Waldner K, et al. Sources and composition of $PM_{2.5}$ at the National Energy Technology Laboratory in Pittsburgh during July and August 2000. Energy Fuel 2002;16:261–9.

Chan CK, Yao XH. Air pollution in mega cities in China. Atmos Environ 2008;42:1–42.

Clegg SL, Brimblecombe P, Wexler AS. Thermodynamic model of the system $H+-NH_4+-Na+-SO_{42}-NO_3-Cl-H_2O$ at 298.15 K. J Phys Chem 1998;102A:2155–71.

Davidson CI, Phalen RF, Solomon PA. Airborne particulate matter and human health: a review. Aerosol Sci Technol 2005;39:737–49.

Draxler RR, Rolph GD. HYSPLIT (hybrid single-particle Lagrangian integrated trajectory) model access via NOAA ARL READY website. Silver Spring, MD: NOAA Air Resources Laboratory; 2003 [Available at: http://www.arl.noaa.gov/HYSPLIT.php (accessed 2009)].

Gao XM, Wang T, Zhou Y, Xue LK, Zhang QZ, Wang XF, et al. Size distribution of atmospheric particles and ware-soluble inorganic ions in spring and summer at Mount Tai. Environ Chem 2010;30:686–92. (in Chinese).

Gao XM, Yang LX, Cheng SH, Gao R, Zhou Y, Xue LK, et al. Semi-continuous measurement of water-soluble ions in $PM_{2.5}$ in Jinan, China: temporal variations and source apportionments. Atmos Environ 2011;45:6048–56.

Guo S, Hu M, Wang ZB, Slanina J, Zhao YL. Size-resolved aerosol water-soluble ionic compositions in the summer of Beijing: implication of regional secondary formation. Atmos Chem Phys 2010;10:947–59.

He KB, Yang FM, Ma YL, Zhang Q, Yao XH, Chan CK, et al. The characteristics of $PM_{2.5}$ in Beijing, China. Atmos Environ 2001;35:4959–70.

Hu M, Wu ZJ, Slanina J, Lin P, Liu S, Zeng LM. Acidic gases, ammonia and water-soluble ions in $PM_{2.5}$ at a coastal site in the Pearl River Delta, China. Atmos Environ 2008;42:6310–20.

Jang M, Czoschke NM, Lee S, Kamens RM. Heterogeneous atmospheric aerosol production by acid-catalyzed particle-phase reactions. Science 2002;298:814–7.

Kido M, Osada K, Matsunaga K, Iwasaka Y. Temporal change in ammonium/sulfate ratios for free tropospheric aerosols from early winter to spring at a high elevation site in the Japanese Alps. J Environ Chem 2001;11:33–41.

Lee TY, Yu XY, Kreidenweis SM, Malm WC, Collett JL. Semi-continuous measurement of $PM_{2.5}$ ionic composition at several rural locations in the United States. Atmos Environ 2008;42:6655–69.

Liu H, Chang WL, Oltmans SJ, Chan LY, Harris JM. On springtime high ozone events in the lower troposphere from Southeast Asian biomass burning. Atmos Environ 1999;33:2403–10.

Mather TA, Allen AG, Oppenheimer C, Pyle DM, Mcgonigle AJS. Size-resolved characterisation of soluble ions in the particles in the tropospheric plume of Masaya Volcano, Nicaragua: origins and plume processing. J Atmos Chem 2003;46:207–37. http://dx.doi.org/10.1023/A:1026327502060.

Ocskay R, Salma I, Wang W, Maenhaut W. Characterization and diurnal variation of size-resolved inorganic water-soluble ions at a rural background site. J Environ Monit 2006;8:300–6.

Qu WJ, Zhang XY, Arimoto R, Wang YQ, Wang D, Sheng LF, Fu G. Aerosol background at two remote CAWNET sites in western China. Sci Total Environ 2009;407:3518–29.

Ram K, Sarin MM, Hegde P. Long-term record of aerosol optical properties and chemical composition from a high-altitude site (Manora Peak) in central Himalaya. Atmos Chem Phys 2010;10:11791–803.

Roger JC, Guinot B, Cachier H, Mallet M, Dubovik O, Yu T. Aerosol complexity in megacities: from size-resolved chemical composition to optical properties of the Beijing atmospheric particles. Geophys Res Lett 2009;36:L18806. http://dx.doi.org/10.1029/2009gl039238.

Seinfeld JH, Pandis SN. Atmospheric chemistry and physics-from air pollution to climate change. 2nd ed. New York: JohnWiley & Sons, Inc.; 2006.

Strader R, Lurmann F, Pandis S. Evaluation of secondary organic aerosol formation in winter. Atmos Environ 1999;33:4849–63.

Sun MH, Wang Y, Wang T, Fan SJ, Wang WX, Li PH, et al. Cloud and the corresponding precipitation chemistry in south China: water-soluble components and pollution transport. J Geophys Res 2010;115:D22303. http://dx.doi.org/10.1029/2010JD014315.

Teinilä K, Hillamo R, Kerminen VW, Beine HJ. Chemistry and modal parameters of major ionic aerosol components during the NICE campaigns at two altitudes. Atmos Environ 2004;38:1481–90.

Underwood GM, Song CH, Phadnis M, Carmichael GR, Grassian VH. Heterogeneous reactions of NO_2 and HNO_3 on oxides and mineral dust: a combined laboratory and modeling study. J Geophys Res 2001;106:18055–66. http://dx.doi.org/10.1029/2000JD900552.

Wang Y, Zhuang GS, Tang AH, Yuan H, Suan YL, Chen S, et al. The ion chemistry and the source of $PM_{2.5}$ aerosol in Beijing. Atmos Environ 2005;39:3771–84.

Wang T, Wong HLA, Tang J, Ding AJ, Gao J, Wu WS, et al. On the origin of surface ozone and reactive nitrogen observed at a remote moutain site in the northeastern Qinghai-Tibetan Plateau, western China. J Geophys Res 2006;111:D08303. http://dx.doi.org/10.1029/2005JD006527.

Wang G, Li J, Cheng C, Hu S, Xie M, Gao S, et al. Observation of atmospheric aerosols at Mt. Hua and Mt. Tai in central and east China during spring 2009 — part 1: EC, OC and inorganic ions. Atmos Chem Phys 2011a;11:4224–35.

Wang Z, Wang T, Gao R, Xue LK, Guo J, Zhou Y, et al. Source and variation of carbonaceous aerosols at Mount Tai, North China: results from a semicontinuous instrument. Atmos Environ 2011b;45:1655–67.

Wang Z, Wang T, Guo J, Gao R, Xue LX, Zhang JM, et al. Formation of secondary organic carbon and cloud impact on carbonaceous aerosols at Mount Tai, North China. Atmos Environ 2012;46:516–27.

Watson JG. Visibility: science and regulation. J Air Waste Manage Assoc 2002;52:628–713.

Xu G, Lee XQ, Lv YC. Urban and rural observations of carboxylic acids in rainwater in Southwest of China: the impact of urbanization. J Atmos Chem 2009;62:249–60.

Xue LK, Wang T, Zhang JM, Zhang XC, Deliger, Poon CN, et al. Source of surface ozone and reactive nitrogen speciation at Mount Waliguan in western China: new insights from the 2006 summer study. J Geophys Res 2011;116:D07306. http://dx.doi.org/10.1029/2010JD014735.

Yang DZ, Yu XL, Fang XM, Wu F, Li XS. A study of aerosol at regional background stations and baseline station. Q J Appl Meteorol 1996;7:396–405. (in Chinese).

Yang F, Tan J, Zhao Q, Du Z, He K, Ma Y, et al. Characteristics of $PM_{2.5}$ speciation in representative megacities and across China. Atmos Chem Phys 2011;11:5207–19.

Yao XH, Chan CK, Fang M, Cadle S, Chan T, Mulawa P, et al. The water-soluble ionic composition of $PM_{2.5}$ in Shanghai and Beijing, China. Atmos Environ 2002;36:4223–34.

Zhang YH, Zhu XL, Slanina S, Shao M, Zeng LM, Hu M, et al. Aerosol pollution in some Chinese cities. Pure Appl Chem 2004;76:1227–39.

Zhang Q, Jimenez JL, Worshop DR, Canagaratna M. A case study of urban particle acidity and its influence on secondary organic aerosol. Environ Sci Technol 2007;41:3213–9.

Zhang Q, Streets DG, Carmichael GR, He KB, Huo H, Kannari A, et al. Asian emissions in 2006 for the NASA INTEX-B mission. Atmos Chem Phys 2009;9:5131–53.

Zhou Y, Wang T, Gao XM, Xue LK, Wang XF, Wang Z, et al. Continuous observations of water-soluble ions in $PM_{2.5}$ at Mount Tai (1534 m a.s.l.) in central-eastern China. J Atmos Chem 2010;64:107–27. http://dx.doi.org/10.1007/s10874-010-9172-z.

Zhou Y, Xue LK, Wang T, Gao XM, Wang Z, Wang XF, et al. Characterization of aerosol acidity at a high mountain site in central eastern China. Atmos Environ 2012;51:11–20.